

# Non- $C_2$ -Symmetric Chiral-at-Ruthenium Catalyst for Highly Efficient Enantioselective Intramolecular $C(sp^3)$ -H Amidation

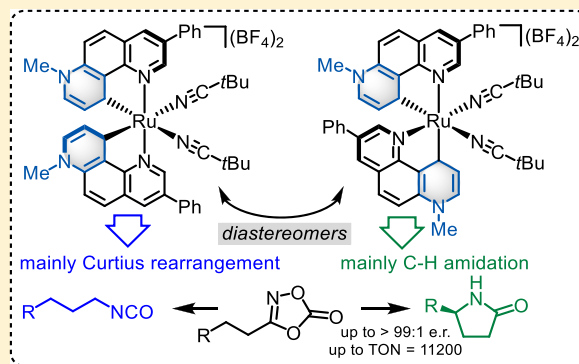
Zijun Zhou,<sup>†,§</sup> Shuming Chen,<sup>‡,§</sup> Yubiao Hong,<sup>†</sup> Erik Winterling,<sup>†</sup> Yuqi Tan,<sup>†</sup> Marcel Hemming,<sup>†</sup> Klaus Harms,<sup>†</sup> K. N. Houk,<sup>\*,‡</sup> and Eric Meggers<sup>\*,†</sup>

<sup>†</sup>Fachbereich Chemie, Philipps-Universität Marburg, Hans-Meerwein-Strasse 4, 35043 Marburg, Germany

<sup>‡</sup>Department of Chemistry and Biochemistry, University of California, Los Angeles, California 90095-1569, United States

## Supporting Information

**ABSTRACT:** A new class of chiral ruthenium catalysts is introduced in which ruthenium is cyclometalated by two 7-methyl-1,7-phenanthroline heterocycles, resulting in chelating pyridylidene remote N-heterocyclic carbene ligands (rNHCs). The overall chirality results from a stereogenic metal center featuring either a  $\Lambda$  or  $\Delta$  absolute configuration. This work features the importance of the relative metal-centered stereochemistry. Only the non- $C_2$ -symmetric chiral-at-ruthenium complexes display unprecedented catalytic activity for the intramolecular  $C(sp^3)$ -H amidation of 1,4,2-dioxazol-5-ones to provide chiral  $\gamma$ -lactams with up to 99:1 er and catalyst loadings down to 0.005 mol % (up to 11 200 TON), while the  $C_2$ -symmetric diastereomer favors an undesired Curtius-type rearrangement. DFT calculations elucidate the origins of the superior C–H amidation reactivity displayed by the non- $C_2$ -symmetric catalysts compared to related  $C_2$ -symmetric counterparts.



## INTRODUCTION

The vast majority of chiral transition metal catalysts contain chiral organic ligands in the coordination sphere of the metal. Recently, we and others demonstrated that effective asymmetric transition metal catalysis does not rely on chiral ligands.<sup>1,2</sup> We introduced a series of chiral transition metal catalysts that are exclusively composed of achiral ligands with the overall chirality being the consequence of a stereogenic metal center. This chiral-at-metal strategy provides untapped opportunities for the design of chiral transition metal catalysts with distinct structural features and electronic properties. However, the current structural variety is limited as, for example, all chiral-at-metal catalysts developed in our laboratory strictly follow the design shown in Scheme 1a, containing two nonsymmetric bidentate and two monodentate ligands coordinated to a central metal in a  $C_2$ -symmetric fashion. The metal-centered configuration  $\Lambda$  versus  $\Delta$  then determines the absolute configuration of the reaction products. A larger structural diversity might lead to more diverse chiral catalysts for a broader variety of asymmetric transformations. For example, one could imagine non- $C_2$ -symmetric diastereomers, expecting that the relative metal-centered stereochemistry affects the overall reactivity of such chiral-at-metal catalysts.

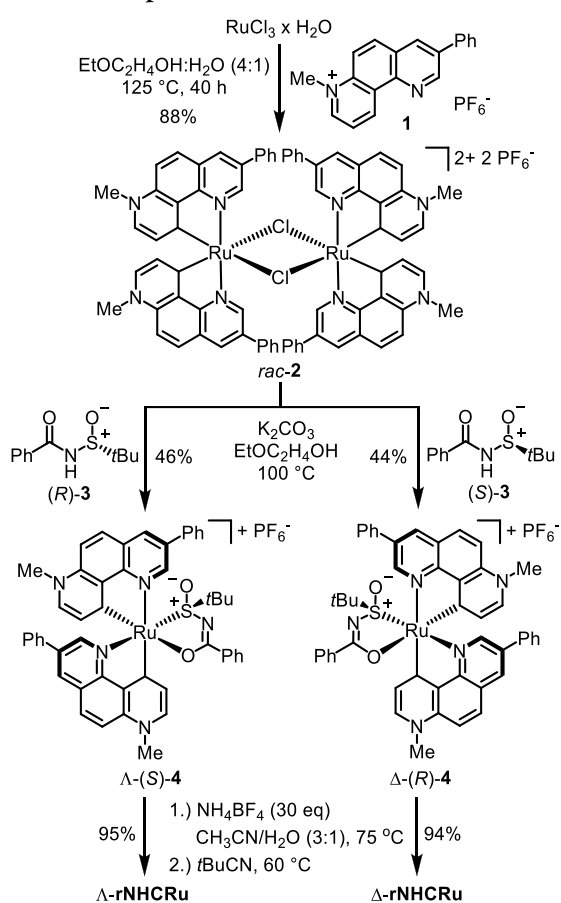
The direct catalytic asymmetric nitrogenation of C–H bonds through a stereocontrolled insertion of metal nitrenoids into prochiral  $C(sp^3)$ -H bonds has emerged as a powerful and economic tool for the efficient synthesis of chiral nonracemic

nitrogen-containing molecules.<sup>6</sup> Recently, Chang introduced a new  $\gamma$ -lactam synthesis through a direct C–H amidation using 1,4,2-dioxazol-5-ones as highly attractive nitrene precursors that can be accessed in two steps (one pot) from ubiquitous carboxylic acids.<sup>7–9</sup> Chang,<sup>10</sup> Yu,<sup>11</sup> and Chen<sup>12</sup> subsequently reported catalytic enantioselective versions of this intramolecular C–H amidation employing well-established chiral half-sandwich iridium or ruthenium complexes (Figure 1b).

However, despite impressive enantioselectivities, these methods along with all other catalytic asymmetric C–H nitrogenations suffer from high catalyst loadings, which renders an application in the pharmaceutical industry unattractive.

Here we introduce a new class of chiral-at-ruthenium catalysts<sup>3,4</sup> containing two strongly electron-donating remote N-heterocyclic carbene (rNHC) ligands<sup>5</sup> coordinated in a non- $C_2$ -symmetric fashion (Figure 1c). The catalyst displays unprecedented catalytic activity for the conversion of 1,4,2-dioxazol-5-ones to chiral  $\gamma$ -lactams at catalyst loadings down to 0.005 mol % (up to 11 200 TON), whereas the  $C_2$ -symmetric diastereomer provides a Curtius-type rearrangement<sup>13</sup> as the main product for the same conversion. Density functional theory (DFT) calculations unravel the role of the ligand architecture for achieving efficient C–H amidations.

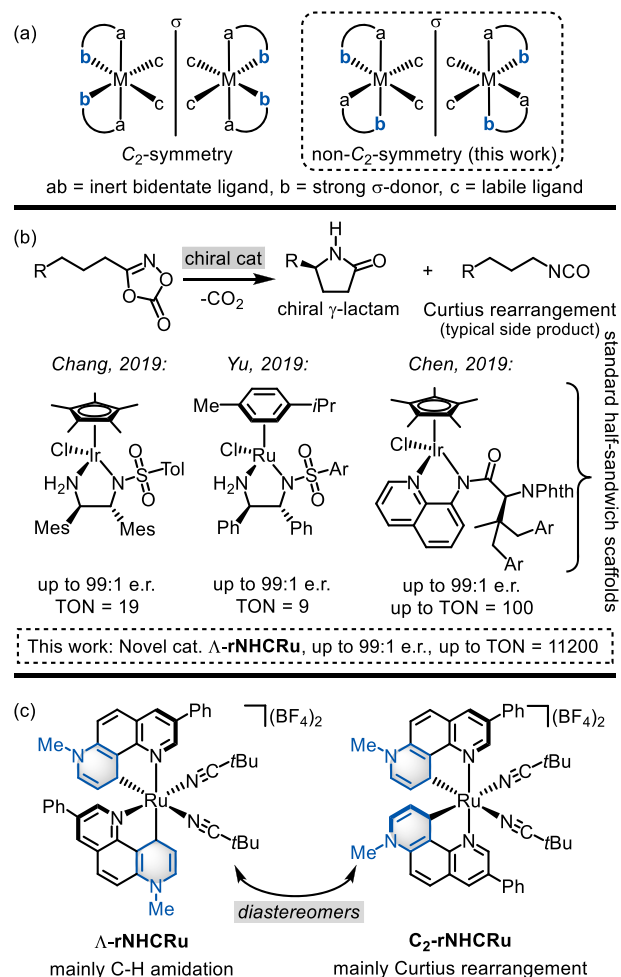
Received: August 28, 2019

Scheme 1. Synthesis of Enantiomerically Pure Chiral-at-Ruthenium Complexes  $\Lambda$ - and  $\Delta$ -rNHCRu

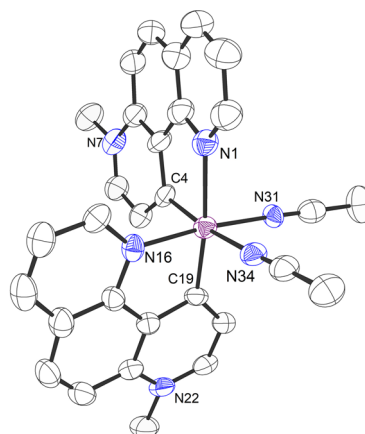
## RESULTS AND DISCUSSION

**Catalyst Design and Synthesis.** Due to the versatile catalytic properties of many ruthenium complexes and the lower cost of ruthenium compared to other platinum-group metals, our laboratory has an active research program developing chiral-at-Ru catalysts. We envisioned achieving high catalytic activity by increasing electron density at the ruthenium center using rNHC ligands. Such rNHC ligands are stronger  $\sigma$ -donors compared to standard NHCs.<sup>5</sup> Accordingly, we chose the heterocycle 7-methyl-3-phenyl-1,7-phenanthroline hexafluorophosphate (**1**) as our ligand of choice (Scheme 1).<sup>14,15</sup> Reaction of RuCl<sub>3</sub> hydrate with **1** in 2-ethoxyethanol/water (4:1) at 125 °C afforded the racemic chloro-bridged dimer complex *rac-2* (88% yield). Each ruthenium is cyclometalated by two 1,7-phenanthroline ligands, which are electronically best described as chelating pyridyl pyridylidene ligands. The racemic mixture was next reacted with (*R*)- or (*S*)-*N*-benzoyl-*tert*-butanesulfinamide (**3**) in the presence of K<sub>2</sub>CO<sub>3</sub> to provide the complexes  $\Lambda$ -(*S*)-**4** or  $\Delta$ -(*R*)-**4** as single stereoisomers in 46% and 44% yield, respectively.<sup>16,17</sup> Interestingly, in the course of the formation of the *N*-sulfinylcarboximidate complexes, an unexpected but important isomerization of the chelating pyridylidene ligands occurred. Treatment with the weak acid NH<sub>4</sub>BF<sub>4</sub> and reaction with pivalonitrile afforded the complexes  $\Lambda$ -rNHCRu and  $\Delta$ -rNHCRu in 95% and 94% yield, respectively.

A crystal structure of a simplified derivative of  $\Lambda$ -rNHCRu, devoid of the two phenyl substituents and bearing two acetonitriles instead of pivalonitriles ( $\Lambda$ -Ru3), is shown in

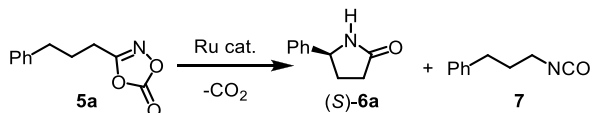
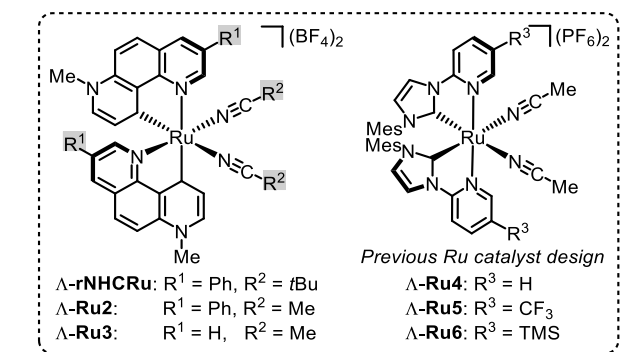


**Figure 1.** Chiral-at-metal complexes and catalysts for enantioselective C(sp<sup>3</sup>)-H amidation. (a) Chiral-at-metal complexes with different symmetry. (b) Catalysts developed in this study. Note that C<sub>2</sub>-rNHCRu was only synthesized as a racemic mixture. (c) Previous studies and this work on enantioselective C(sp<sup>3</sup>)-H amidations with 1,4,2-dioxazol-5-ones.



**Figure 2.** Single-crystal X-ray structure of  $\Lambda$ -Ru3, a derivative of  $\Lambda$ -rNHCRu (CCDC 1910816). ORTEP drawing with 50% probability thermal ellipsoids. Solvent and counterion are omitted for clarity.

Figure 2 and was used to assign the relative and absolute metal-centered stereochemistry. It is noteworthy that due to the lacking C<sub>2</sub>-symmetry of this complex, the two coordinated

Table 1. Comparison of Different Ruthenium Catalysts<sup>a</sup>

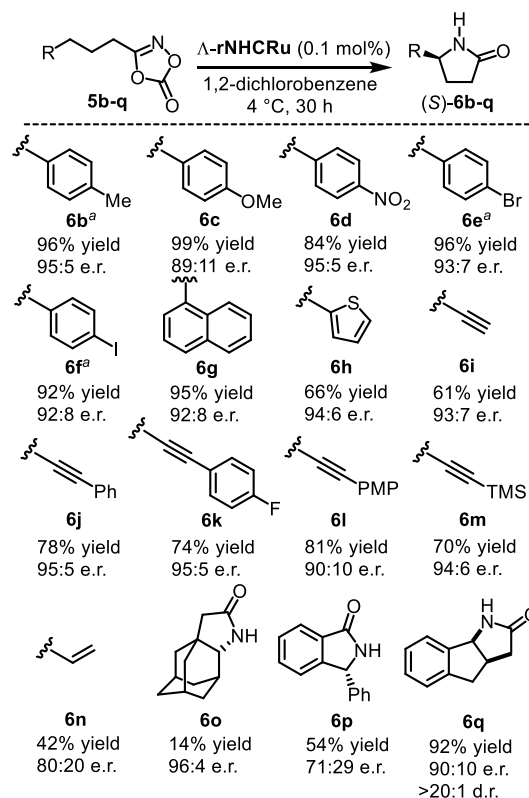
entry	catalyst	loading (mol %)	T (°C)	yield (%) <sup>b</sup>		
				6a	7	er <sup>c</sup>
1	$\Lambda$ - <b>rNHCRu</b>	0.5	rt	93 (92) <sup>d</sup>	6	95:5
2	$\Lambda$ - <b>Ru2</b>	0.5	rt	92 (91) <sup>d</sup>	7	94:6
3	$\Lambda$ - <b>Ru3</b>	0.5	rt	84 (82) <sup>d</sup>	15	92:8
4	$\Lambda$ - <b>Ru4</b>	0.5	rt	>99		
5	$\Lambda$ - <b>Ru5</b>	0.5	rt	>99		
6	$\Lambda$ - <b>Ru6</b>	0.5	rt	>99		
7	$\Lambda$ - <b>rNHCRu</b>	0.5	4	95 (95) <sup>d</sup>	5	96:4
8 <sup>e</sup>	$\Lambda$ - <b>rNHCRu</b>	0.1	4	95 (95) <sup>d</sup>	5	96:4
9 <sup>f</sup>	$\Lambda$ - <b>rNHCRu</b>	0.05	4	93 (93) <sup>d</sup>	7	95:5

<sup>a</sup>Standard conditions: **5** (0.2 mmol) and Ru catalyst (0.05–0.5 mol %) in 1,2-dichlorobenzene (0.4 mL) stirred at the indicated temperature for 8 h under an atmosphere of nitrogen. <sup>b</sup>Yields based on <sup>1</sup>H NMR analysis. <sup>c</sup>Enantiomeric ratio of the crude product determined by HPLC analysis on a chiral stationary phase. <sup>d</sup>Isolated yields in brackets. <sup>e</sup>Reaction time of 30 h instead. <sup>f</sup>Reaction time of 48 h instead.

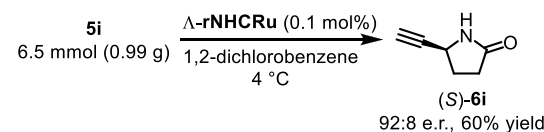
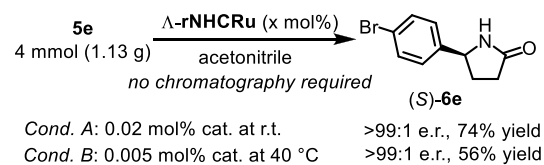
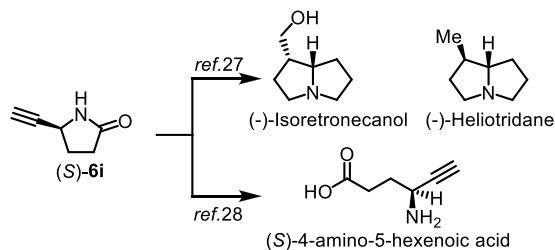
nitriles are not equivalent. The strong  $\sigma$ -donating pyridylidene ligand renders the acetonitrile ligand in *trans* position more labile, which is evident from an elongated coordinative bond (Ru1–N34 = 2.115 Å as compared to Ru1–N31 = 2.002 Å).<sup>18</sup> To our knowledge, this is the first example of ruthenium cyclometalated by two 7-alkyl-1,7-phenanthroline ions.<sup>19</sup>

**Initial Experiments on Enantioselective C(sp<sup>3</sup>)–H Amidations.** We investigated the catalytic properties of the new chiral-at-ruthenium complex and found that  $\Lambda$ -**rNHCRu** displays excellent catalytic activity for the intramolecular C–H amidation of 1,4,2-dioxazol-5-ones. For example, using just 0.5 mol % of  $\Lambda$ -**rNHCRu** at room temperature catalyzed the conversion of **5a** to the  $\gamma$ -lactam (**S**)-**6a** in 92% yield and with 95:5 er (Table 1, entry 1). The related catalysts  $\Lambda$ -**Ru2** (acetonitriles instead of pivalonitriles) and  $\Lambda$ -**Ru3** (devoid of phenyl groups and acetonitriles instead of pivalonitriles) provided lower yields and enantioselectivities for this conversion and higher yields of side product isocyanate formation (entries 2 and 3). Importantly, our previous chiral-at-ruthenium complexes **Ru4**–**Ru6**, which were demonstrated to be very suitable catalysts for enantioselective C–H aminations of aliphatic azides,<sup>20,21</sup> did not afford any detectable amounts of the C–H amidation product but instead quantitatively provided the isocyanate compound **7** (entries 4–6). Thus, **rNHCRu** has very distinct catalytic

Scheme 2. Substrate Scope



<sup>a</sup>Reactions performed in acetonitrile at room temperature for 8 h instead of standard conditions.

Scheme 3. Gram-Scale Reaction with Low Catalyst Loading and Further Transformations: (a) Gram-Scale Synthesis of (**S**)-**6e** and (**S**)-**6i**; (b) Synthetic Applications of (**S**)-**6i**(a) Gram-scale synthesis of (**S**)-**6e** and (**S**)-**6i**:(b) Product transformations of (**S**)-**6i**:

properties. The yield and enantioselectivity of **rNHCRu**-catalyzed conversion **5a**  $\rightarrow$  (**S**)-**6a** can be further improved to 95% yield and 96:4 er by performing the reaction at 4 °C. To demonstrate the exceptional catalytic activity of **rNHCRu**,

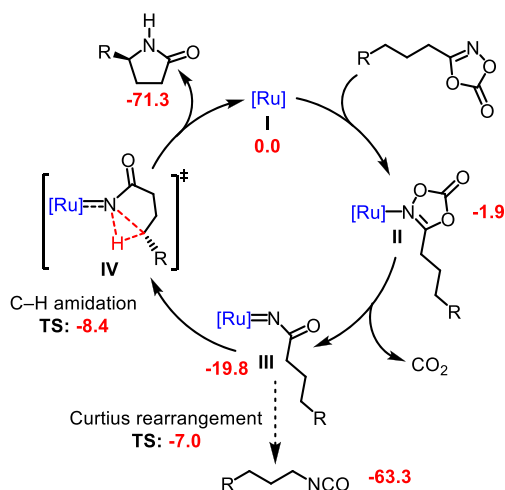
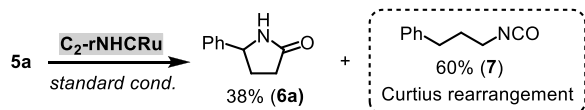


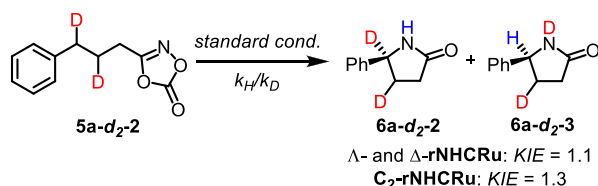
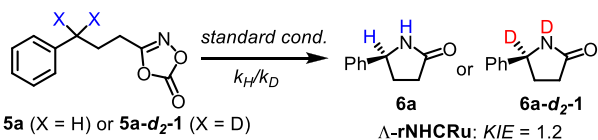
**Figure 3.** Proposed mechanism and calculated free energies (kcal/mol) at the M06-D3/6-311++G(d,p)-SDD (Ru), SMD (1,2-dichlorobenzene)//B3LYP-D3/6-31G(d)-LANL2DZ (Ru) level of theory, with Ru2 as the catalyst and 5a as the substrate (see Supporting Information).

#### Scheme 4. Control Experiments for Elucidating the Mechanism

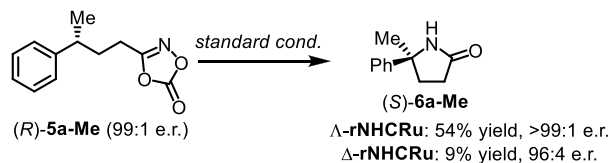
##### (a) Control experiment with C<sub>2</sub>-symmetric rNHCRu:



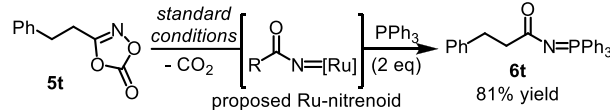
##### (b) Kinetic isotope effects:



##### (c) Probing the stereochemistry:



##### (d) Trapping of Ru-nitrenoid intermediate:



catalyst loading was further reduced (entries 7–9). At a catalyst loading of just 0.05 mol % the intramolecular C–H amidation still occurred with 93% yield and 95:5 er.

**Substrate Scope.** With the optimized catalyst and reaction conditions in hand, we performed a substrate scope (Scheme 2). A methyl group in *para*-position of the phenyl moiety was well tolerated and provided 96% yield with 95:5 er (6b). An electron-donating methoxy group in the *para*-position of the

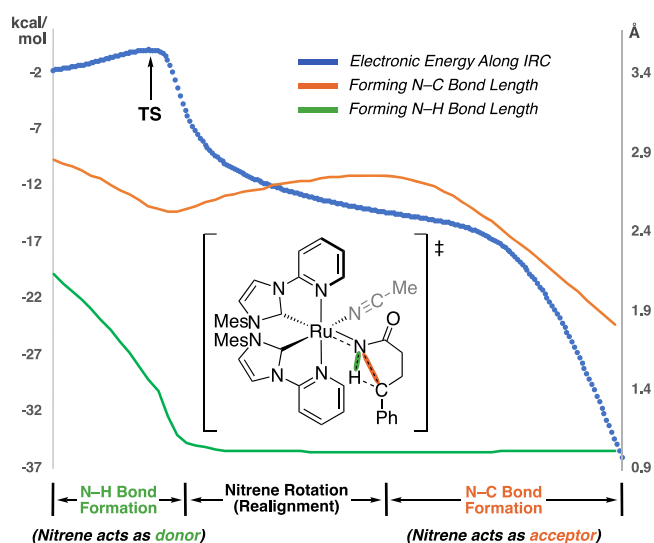


**Figure 4.** Calculated electronic energy and forming bond lengths along the IRC of the C–H amidation reaction catalyzed by Ru4 at the B3LYP-D3/6-31G(d)-LANL2DZ (Ru) level of theory.

phenyl moiety provided an almost quantitative yield but with a reduced enantioselectivity (6c). An electron-withdrawing nitro substituent at the *para*-position of the phenyl moiety gave 84% yield with 95:5 er (6d). Halogen substituents at the *para*-position of the phenyl moiety were also well tolerated and provided high yields and good enantioselectivities (6e, 6f). Of note, both the brominated (6e) and iodinated (6f)  $\gamma$ -lactam products were improved to >99:1 er after a single recrystallization in ethyl acetate (see SI for details).<sup>22</sup> Replacing the phenyl moiety with a sterically more demanding naphthyl moiety provided the desired lactam product (6g) with 95% yield and 92:8 er. A substrate with the heteroaromatic thiophene (6h) afforded a lower yield with 94:6 er.

Next, we performed reactions of 1,4,2-dioxazol-5-ones with alkynyl substituents adjacent to the  $\gamma$ -C–H group, which afforded chiral  $\gamma$ -alkynyl lactams in 61–81% yield and with up to 95:5 er (6i–m). It is noteworthy that a terminal alkyne ( $\gamma$ -lactam 6i) and trimethylsilyl (TMS)-functionalized alkyne ( $\gamma$ -lactam 6m) were not included in previous reports on the direct enantioselective C–H amidation using 1,4,2-dioxazol-5-ones.<sup>10–12</sup> Finally, with respect to substrate scope, a vinyl group next to the  $\gamma$ -C–H afforded the  $\gamma$ -vinyl lactam 6n with modest 42% yield and 80:20 er. If the  $\gamma$ -C–H is not activated by a  $\pi$ -system, the yields are low, as shown for the adamantyl product 6o.<sup>23</sup> The synthesis of a chiral isoindolinone (6p) and a desymmetrization generating two stereocenters (6q) are also shown in Scheme 2.

#### Gram-Scale Reactions and Synthetic Applications.

The practical value of our developed C–H amidation catalyst was demonstrated in a gram-scale synthesis of (S)-6e with a catalyst loading of 0.02 mol % (Scheme 3a). Interestingly, the isolation of the desired C–H amidation product was performed without column chromatography by only precipitation<sup>24</sup> and crystallization in 74% yield and with >99:1 er. It is noteworthy that the catalyst loading can be further reduced to merely 0.005 mol % to provide (S)-6e with 56% yield and >99:1 er (TON number = 11 200) at the same reaction scale.<sup>25</sup> We believe this is the highest TON number reported for asymmetric transition metal complex catalyzed ring-closing C–

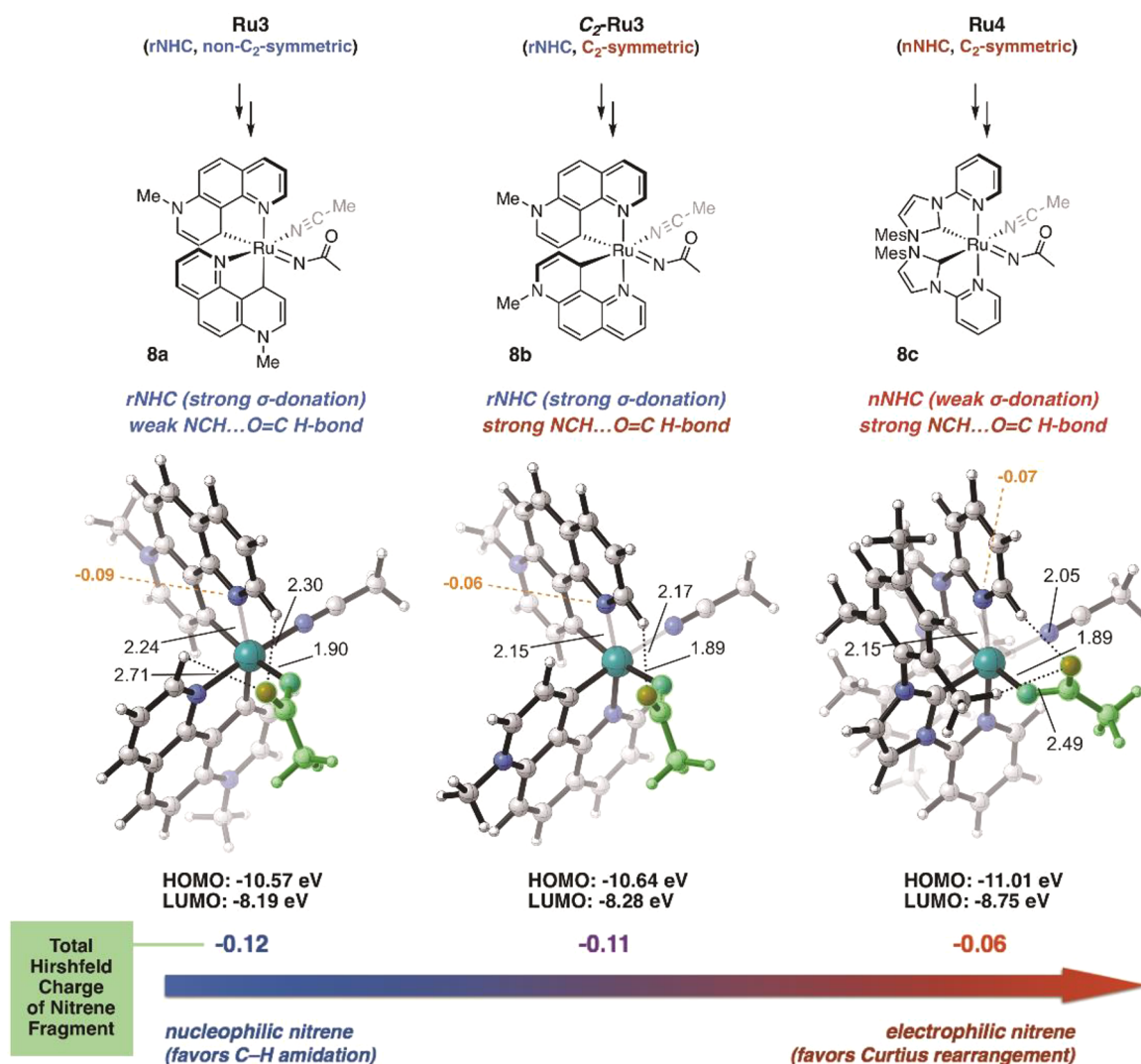


**Figure 5.** Calculated structures of ruthenium nitrene complexes at the B3LYP-D3/6-31G(d)-LANL2DZ (Ru) level of theory. Interatomic distances are in angstroms (Å). Bolded numbers in orange indicate Hirshfeld charges on individual atoms.

H nitrogenations. A gram-scale synthesis was also demonstrated for the terminal alkyne-functionalized  $\gamma$ -lactam (*S*)-**6i**, obtained in 60% yield with 92:8 er.

Chiral  $\gamma$ -lactams are useful intermediates for the synthesis of bioactive molecules such as natural products and drugs. For example, the  $\gamma$ -lactam (*R*)-**6e** has been reported as an intermediate for the synthesis of a compound for the treatment of inflammatory disorders and a hydroxamate-based inhibitor of deacetylases B.<sup>26</sup> Chiral  $\gamma$ -lactam (*S*)-**6i**, containing a terminal alkyne, was reported as a synthetic intermediate used in the total syntheses of the natural products (–)-isoretrocanol, (–)-heliotridane,<sup>27</sup> and the GABA aminotransferase and glutamic acid decarboxylase inhibitor (*S*)-(+)-4-amino-5-hexynoic acid<sup>28</sup> (Scheme 3b). (*S*)-**6i** was previously synthesized in multiple steps starting from chiral amino acids or amino esters.<sup>27,28</sup>

**Mechanistic Studies.** The proposed mechanism is shown in Figure 3. The reaction is initiated by ruthenium (I) coordination to the 1,4,2-dioxazol-5-one (intermediate II). A subsequent fragmentation and release of CO<sub>2</sub> gas generates the ruthenium-imido intermediate III, followed by stereocontrolled insertion of the nitrene moiety into the C–H bond

(IV), and subsequent release of the lactam product finishes the whole catalytic cycle.

We started our mechanistic study by investigating the influence of the relative stereochemistry of the new ruthenium catalyst scaffold on promoting C–H amidation reactivity. The complex rNHCru features non- $C_2$ -symmetry, whereas all catalysts previously developed in our group for asymmetric C–H aminations (Ru4–Ru6) display  $C_2$ -symmetry, but only provide the undesired Curtius-type rearrangement products (Table 1, entries 4–6). To evaluate the importance of the relative stereochemistry around the metal center and the potential electronic role of the rNHC ligands, we synthesized the  $C_2$ -symmetric diastereomer of rNHCru ( $C_2$ -rNHCru, Figure 1c) and subjected it to standard reaction conditions with dioxazolone **5a**. Revealingly, the Curtius-type rearrangement product **7** was formed as the major reaction product in 60% yield with only 38% C–H amidation, demonstrating that the relative stereochemistry of rNHCru has a significant effect on the reaction outcome (Scheme 4a).

An intermolecular KIE value of 1.2 was determined by measuring initial C–H amidation rates of nondeuterated and bis-deuterated substrates (Scheme 4b).<sup>29</sup> The C–H amidations with a substrate bearing a benzylic-CHD stereocenter

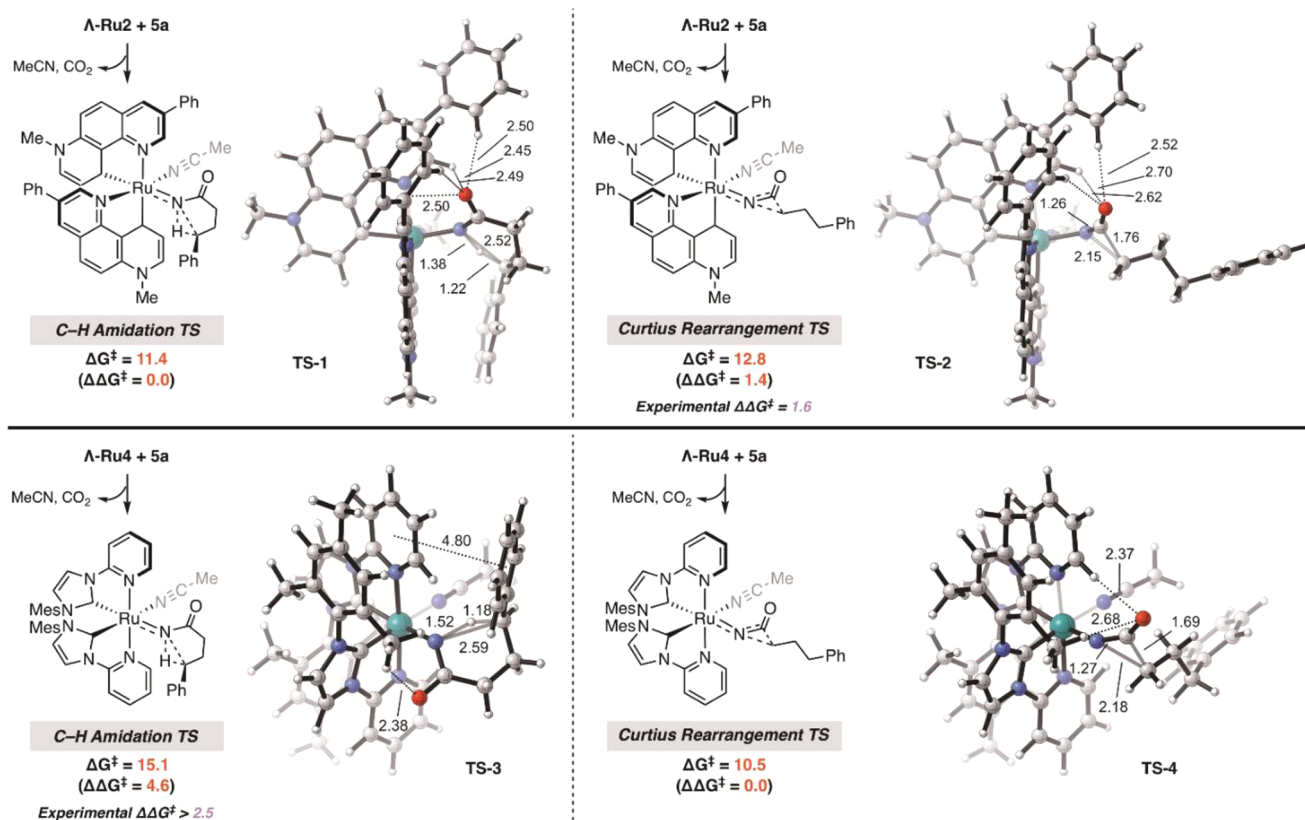


**Figure 6.** Calculated C–H amidation and Curtius rearrangement transition states at the M06-D3/6-311++G(d,p)–SDD (Ru), SMD (1,2-dichlorobenzene)//B3LYP-D3/6-31G(d)–LANL2DZ (Ru) level of theory. Interatomic distances are in angstroms (Å). Energies are in kcal/mol. Activation barriers are calculated with respect to the lowest-energy conformers of Ru nitrene intermediate **III**.

were tested by using different **rNHCRu** catalysts. Both  $\Lambda$ - or  $\Delta$ -**rNHCRu** gave a KIE value of 1.1, while  $C_2$ -**rNHCRu**, the  $C_2$ -symmetric diastereomer of **rNHCRu**, afforded a KIE value of 1.3. Low KIE values were also obtained in related work by Chang, Yu, and Chen using dioxazolones as nitrene precursors.<sup>7,10–12</sup> These results indicate a singlet nitrene insertion with a concerted N–C and N–H formation pathway,<sup>30</sup> although a stepwise radical reaction through a triplet nitrene cannot be totally excluded. We also tested the stereochemistry of the reaction by subjecting the nonracemic (99:1 er) chiral substrate (*R*)-**5a-Me** to the C–H amidation conditions. As a result, (*S*)-**6a-Me** with retention of configuration at the reacted carbon was obtained as the major product with both  $\Lambda$ - and  $\Delta$ -**rNHCRu**, but the  $\Lambda$ -catalyst reacts significantly faster with higher yield and affords the  $\gamma$ -lactam with a higher enantiomeric excess, thus revealing a high stereochemical discrimination between the two enantiotopic C–H bonds (Scheme 4c).

Transition metal nitrenoids have been reported to transfer the nitrene fragment to phosphines to furnish iminophosphoranes.<sup>31</sup> To gain experimental evidence for the formation of an intermediate ruthenium nitrenoid in our catalytic system, we performed a trapping experiment with  $\text{PPh}_3$  using a dioxazolone substrate (**5t**) that is not capable of undergoing an intramolecular  $\delta$ -C–H insertion (Scheme 4d). As a result, the expected iminophosphorane **6t** was formed in 81% yield under our standard reaction conditions, which is consistent with our assumption that the ruthenium-catalyzed reaction proceeds through an intermediate ruthenium nitrenoid.

To reveal how the non- $C_2$ -symmetric catalysts improve selectivity for the desired C–H amidation pathway over the undesired Curtius rearrangement, we performed DFT calculations. The electrophilicity of the nitrene fragment is expected to be an important factor in determining C–H amidation versus Curtius rearrangement reactivity. Curtius rearrangements favor electrophilic nitrenes and are well-known to be catalyzed by Lewis or Brønsted acids.<sup>32,33</sup> The C–H amidation pathway, on the other hand, requires more nucleophilic nitrenes due to its concerted but asynchronous nature. The calculated intrinsic reaction coordinate (IRC) for the C–H amidation catalyzed by **Ru4** shows that the N–H bond formation occurs first, driven by nitrene lone pair donation into  $\sigma^*_{\text{C–H}}$  (Figure 4). This is followed by rotation of the nitrene moiety to align its empty p orbital with the deprotonated nucleophilic carbon, which allows the N–C bond to form. A more electron-rich nitrene with stronger donor ability is therefore essential for lowering the C–H amidation barrier.<sup>7</sup>

Calculated structures of ruthenium *N*-acylnitrenes (**8a–c**) formed with the three model catalysts **Ru3**, its  $C_2$ -symmetric diastereomer  $C_2$ -**Ru3**, and **Ru4** are shown in Figure 5. Both **Ru3** and  $C_2$ -**Ru3** bear **rNHC** ligands, while **Ru4** has normal NHC (nNHC) ligands. Hirshfeld charge analysis shows that **rNHC**-bearing **8a** (from **Ru3**) and **8b** (from  $C_2$ -**Ru3**) have more electron-rich nitrene fragments (highlighted in green) than **8c**.<sup>34</sup> This is consistent with the expected higher  $\sigma$ -donating ability of **rNHC** over nNHC ligands.<sup>5</sup> The calculated structures also reveal another factor that influences the electron-richness of the nitrenes, namely,  $\text{NCH}\cdots\text{O}=\text{C}$

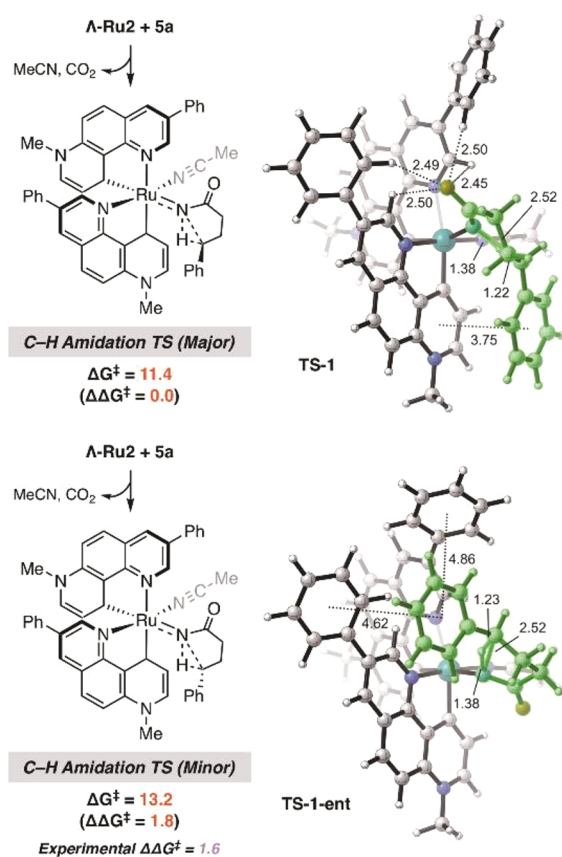


**Figure 7.** Calculated C–H amidation transition states leading to major and minor lactam enantiomers at the M06-D3/6-311++G(d,p)–SDD (Ru), SMD (1,2-dichlorobenzene)//B3LYP-D3/6-31G(d)–LANL2DZ (Ru) level of theory. Interatomic distances are in angstroms (Å). Energies are in kcal/mol. Activation barriers are calculated with respect to the lowest-energy conformer of Ru nitrene intermediate III.

hydrogen bonds between the carbonyl group of the acylnitrene and the polarized C–H bond in 2-position of the closeby pyridyl ligand. This  $\text{NCH}\cdots\text{O}=\text{C}$  hydrogen bond is significantly stronger in **8b** (2.17 Å) and **8c** (2.05 Å), which are both derived from  $C_2$ -symmetric catalysts, than in **8a** (2.30 Å) derived from a non- $C_2$ -symmetric catalyst. In **8a**, the metal's coordination bond to one of the pyridine nitrogens is lengthened (2.24 Å, versus 2.15 Å in **8b** and **8c**) due to being positioned *trans* to the strongly  $\sigma$ -donating rNHC carbene carbon.<sup>35,36</sup> The longer Ru–N(pyridine) bond leads to a more electron-rich pyridine nitrogen and a less acidic  $\alpha$ -CH bond, which consequently weakens the  $\text{NCH}\cdots\text{O}=\text{C}$  hydrogen bond in **8a** over **8b** and **8c**. Both Hirshfeld charges and orbital energies (see Figure 5) show that the overall nucleophilicity of the nitrene fragment decreases in the order of **8a** > **8b** > **8c**, predicting that rNHC-bearing, non- $C_2$ -symmetric catalysts should be the most selective for C–H amidation, in agreement with the experimental results (Table 1, entries 1–3).

Figure 6 shows the calculated transition states for the C–H amidation and Curtius rearrangement with substrate **5a** and the catalysts **Ru2** (non- $C_2$ -symmetry) and **Ru4** ( $C_2$ -symmetry). For **Ru2**, C–H amidation proceeds with a barrier of 11.4 kcal/mol, 1.4 kcal/mol lower than for the Curtius rearrangement pathway. This result is in excellent agreement with the experimentally observed product ratio (**6a**:**7** = 92:7,  $\Delta\Delta G^\ddagger =$

1.6 kcal/mol). For **Ru4**, Curtius rearrangement is more facile with a barrier of 10.5 kcal/mol, while the C–H amidation barrier increases to 15.1 kcal/mol. The large  $\Delta\Delta G^\ddagger$  of 4.6 kcal/mol is consistent with the experimental observation that **Ru4** leads exclusively to the Curtius rearrangement product.

Aside from higher nitrene electrophilicity, we hypothesized that steric factors may also play a role. In **Ru4** two mesityl groups are in close vicinity to the active site and may disfavor C–H amidation because of the more sterically demanding transition state, in which the nitrene alkyl chain must fold into a particular conformation in order to cyclize. To assess the role of steric effects, we calculated the C–H amidation and Curtius rearrangement transition states for **Ru4-Me**, a modified version of **Ru4** in which the large *N*-Mes groups are replaced with sterically less demanding *N*-Me groups (see Supporting Information). Surprisingly, the Curtius rearrangement pathway is still favored by 4.3 kcal/mol, only 0.3 kcal/mol less than for **Ru4**. These results indicate that nitrene electrophilicity and not sterics is the dominant factor in determining C–H amidation versus Curtius rearrangement selectivity.<sup>37</sup>

Finally, we calculated C–H amidation transition states for the reaction **5a**  $\rightarrow$  **6a** catalyzed by  $\Lambda$ -**Ru2**, leading to different enantiomers of the lactam product (Figure 7). **TS-1**, which leads to the major enantiomer (*S*)-**6a**, is favored by 1.8 kcal/mol, in good agreement with the observed er of 94:6 ( $\Delta\Delta G^\ddagger = 1.6$  kcal/mol). A stabilizing  $\pi$ – $\pi$  stacking interaction exists between the nitrene phenyl group and the rNHC ligand. In **TS-1-ent**, the cyclizing nitrene fragment is oriented quite differently, with two weaker  $\pi$ – $\pi$  stacking interactions between the nitrene phenyl group and the phenyl substituents on the rNHC ligands.

Our calculations also established the energetic feasibility of the proposed catalytic cycle (Figure 3). After coordination of the substrate to the Ru center, extrusion of  $\text{CO}_2$  to furnish **III** is exergonic (–17.9 kcal/mol for **Ru2** and **5a**). Both C–H amidation and Curtius rearrangement pathways have low barriers, consistent with the observation that the reactions generally proceed at room temperature or below.

## CONCLUSIONS

In conclusion, we have introduced a new class of chiral ruthenium catalysts and have elucidated the role of the relative metal-centered configuration and electronic characteristics of the coordinated rNHC ligands for catalytic activity. The non- $C_2$ -symmetric scaffold exhibits a unique core structure with two chelating pyridylidene remote NHC ligands that provide high electron density at the ruthenium and at the same time are responsible for the overall chirality through a helical arrangement in the coordination sphere. The catalyst rNHCru shows an exceptional catalytic activity for the enantioselective C–H amidation of 1,4,2-dioxazol-5-ones to chiral  $\gamma$ -lactams, reaching TONs of up to 11 200 (0.005 mol % catalyst loading). We believe that such a low catalyst loading is unprecedented for enantioselective C–H nitrogenations with nonenzymatic catalysts.<sup>38</sup> Interestingly, the  $C_2$ -symmetric diastereomer of rNHCru, as well as previously reported  $C_2$ -symmetric ruthenium catalysts suitable for enantioselective C–H aminations, provides instead an undesired Curtius-type rearrangement as the main product. DFT calculations reveal that the combination of strongly electron-donating remote NHC ligands and the non- $C_2$ -symmetric arrangement of these ligands in the coordination sphere provides an especially electron-rich ruthenium nitrene intermediate favorable for an

efficient C–H amidation step. In this catalyst architecture, the relative metal-centered stereochemistry (non- $C_2$ - vs  $C_2$ -symmetry) is therefore crucial for the reactivity and fate of the catalyzed reaction, while the absolute metal-centered stereochemistry ( $\Lambda$  vs  $\Delta$ ) determines the absolute configuration of the C–H amidation product. Thus, whereas  $C_2$ -symmetric chiral transition metal catalysts are typically desirable for reducing the number of competing processes and transition states, in this catalyst architecture only the diastereomer with lower symmetry provides the desired catalytic activity. Future work will investigate other chiral ruthenium catalyst architectures with decreased symmetry for applications in asymmetric catalysis.

## ■ ASSOCIATED CONTENT

### Supporting Information

The Supporting Information is available free of charge at <https://pubs.acs.org/doi/10.1021/jacs.9b09301>.

Experimental procedures, compound characterization data, NMR spectra, HPLC traces, crystallographic data, and details of the computational study (PDF)

Crystallographic data for (S)-**6e** (CIF)

Crystallographic data for  $\Lambda$ -**Ru3** (CIF)

Crystallographic data for  $\Lambda$ -(S)-**S12** (CIF)

## ■ AUTHOR INFORMATION

### Corresponding Authors

\*[hok@chem.ucla.edu](mailto:hok@chem.ucla.edu)

\*[meggers@chemie.uni-marburg.de](mailto:meggers@chemie.uni-marburg.de)

### ORCID

Shuming Chen: 0000-0003-1897-2249

K. N. Houk: 0000-0002-8387-5261

Eric Meggers: 0000-0002-8851-7623

### Author Contributions

<sup>§</sup>Z.Z. and S.C. contributed equally.

### Notes

The authors declare no competing financial interest.

Crystallographic data for (S)-**6e**,  $\Lambda$ -**Ru3**, and  $\Lambda$ -(S)-**S12** have been deposited with the Cambridge Crystallographic Data Centre as supplementary publication numbers CCDC 1910815, 1910816, and 1910817, respectively.

## ■ ACKNOWLEDGMENTS

E.M. gratefully acknowledges funding from the Deutsche Forschungsgemeinschaft (ME 1805/15-1). K.N.H. is grateful to the National Science Foundation (Grant CHE-1764328) for financial support. Calculations were performed on the Hoffman2 cluster at the University of California, Los Angeles, and the Extreme Science and Engineering Discovery Environment (XSEDE), which is supported by the National Science Foundation (Grant OCI-1053575).

## ■ REFERENCES

- (1) Zhang, L.; Meggers, E. Stereogenic-only-at-metal asymmetric catalysts. *Chem. - Asian J.* **2017**, *12*, 2335.
- (2) Zhang, L.; Meggers, E. Steering asymmetric Lewis acid catalysis exclusively with octahedral metal-centered chirality. *Acc. Chem. Res.* **2017**, *50*, 320.
- (3) Hartung, J.; Grubbs, R. H. Highly Z-selective and enantioselective ring-opening/cross-metathesis catalyzed by a resolved stereo-given-at-Ru complex. *J. Am. Chem. Soc.* **2013**, *135*, 10183.

- (4) Zheng, Y.; Tan, Y.; Harms, K.; Marsch, M.; Riedel, R.; Zhang, L.; Meggers, E. Octahedral ruthenium complex with exclusive metal-centered chirality for highly effective asymmetric catalysis. *J. Am. Chem. Soc.* **2017**, *139*, 4322.

- (5) (a) Raubenheimer, H. G.; Cronje, S. One-N, six-membered heterocyclic carbene complexes and the remote heteroatom concept. *Dalton Trans.* **2008**, 1265. (b) Crabtree, R. H. Abnormal, mesoionic and remote N-heterocyclic carbene complexes. *Coord. Chem. Rev.* **2013**, *257*, 755. (c) Vivancos, Á.; Segarra, C.; Albrecht, M. Mesoionic and related less heteroatom-stabilized N-heterocyclic carbene complexes: Synthesis, catalysis, and other applications. *Chem. Rev.* **2018**, *118*, 9493.

- (6) (a) Espino, C. G.; Fiori, K. W.; Kim, M.; Du Bois, J. Expanding the scope of C–H amination through catalyst design. *J. Am. Chem. Soc.* **2004**, *126*, 15378. (b) Collet, F.; Dodd, R. H.; Dauban, P. Catalytic C–H amination: recent progress and future directions. *Chem. Commun.* **2009**, 5061. (c) Zalatan, D. N.; Du Bois, J. Understanding the differential performance of  $Rh_2(esp)_2$  as a catalyst for C–H amination. *J. Am. Chem. Soc.* **2009**, *131*, 7558. (d) Driver, T. G. Recent advances in transition metal-catalyzed N-atom transfer reactions of azides. *Org. Biomol. Chem.* **2010**, *8*, 3831. (e) Collet, F.; Lescot, C.; Dauban, P. Catalytic C–H amination: the stereoselectivity issue. *Chem. Soc. Rev.* **2011**, *40*, 1926. (f) Che, C.-M.; Lo, V. K.-Y.; Zhou, C.-Y.; Huang, J.-S. Selective functionalisation of saturated C-H bonds with metalloporphyrin catalysts. *Chem. Soc. Rev.* **2011**, *40*, 1950. (g) Roizen, J. L.; Harvey, M. E.; Du Bois, J. Metal-catalyzed nitrogen-atom transfer methods for the oxidation of aliphatic C–H bonds. *Acc. Chem. Res.* **2012**, *45*, 911. (h) Dequierez, G.; Pons, V.; Dauban, P. Nitrene chemistry in organic synthesis: Still in its infancy? *Angew. Chem., Int. Ed.* **2012**, *51*, 7384. (i) Darses, B.; Rodrigues, R.; Neuville, L.; Mazurais, M.; Dauban, P. Transition metal-catalyzed iodine(III)-mediated nitrene transfer reactions: efficient tools for challenging syntheses. *Chem. Commun.* **2017**, 53, 493. (j) Hazelard, D.; Nocquet, P.-A.; Compain, P. Catalytic C–H amination at its limits: challenges and solutions. *Org. Chem. Front.* **2017**, *4*, 2500. (k) Park, Y.; Kim, Y.; Chang, S. Transition metal-catalyzed C–H amination: Scope, mechanism, and applications. *Chem. Rev.* **2017**, *117*, 9247.

- (7) Hong, S. Y.; Park, Y.; Hwang, Y.; Kim, Y. B.; Baik, M.-H.; Chang, S. Selective formation of  $\gamma$ -lactams via C–H amidation enabled by tailored iridium catalysts. *Science* **2018**, *359*, 1016.

- (8) For 1,4,2-dioxazol-5-one as nitrene precursor for intermolecular allylic C–H amidations, see: (a) Lei, H.; Rovis, T. Ir-catalyzed intermolecular branch-selective allylic C–H amidation of unactivated terminal olefins. *J. Am. Chem. Soc.* **2019**, *141*, 2268. (b) Knecht, T.; Mondal, S.; Ye, Y.; Das, M.; Glorius, F. Intermolecular, branch-selective, and redox neutral  $Cp^*Ir^{III}$ -catalyzed allylic C–H amidation. *Angew. Chem., Int. Ed.* **2019**, *58*, 7117. (c) Burman, J. S.; Harris, R. J.; Farr, C. M. B.; Bacsá, J.; Blakey, S. B. Rh(III) and Ir(III) $Cp^*$  complexes provide complementary regioselectivity profiles in intermolecular allylic C–H amidation reactions. *ACS Catal.* **2019**, *9*, 5474.

- (9) For earlier work on utilizing 1,4,2-dioxazol-5-ones as nitrene precursors, see: (a) Zhong, C. L.; Tang, B. Y.; Yin, P.; Chen, Y.; He, L. Synthesis of 2,5-disubstituted oxazoles and oxazolones catalyzed by ruthenium(II) porphyrin and simple copper salts. *J. Org. Chem.* **2012**, *77*, 4271. (b) Bizet, V.; Buglioni, L.; Bolm, C. Light-induced ruthenium-catalyzed nitrene transfer reactions: a photochemical approach towards N-acyl sulfimides and sulfoximines. *Angew. Chem., Int. Ed.* **2014**, *53*, 5639. (c) Wang, H.; Tang, G.-D.; Li, X.-W. Rhodium(III)-catalyzed amidation of unactivated C(sp<sup>3</sup>)-H bonds. *Angew. Chem., Int. Ed.* **2015**, *54*, 13049. (d) Wang, F.; Jin, L.; Kong, L.; Li, X.-W. Cobalt(III)- and Rhodium(III)-catalyzed C–H amidation and synthesis of 4-quinolones: C–H activation assisted by weakly coordinating and functionalizable enamino. *Org. Lett.* **2017**, *19*, 1812. (e) Hermann, G. H.; Bolm, C. Mechanochemical rhodium(III)-catalyzed C–H bond amidation of arenes with dioxazolones under solventless conditions in a ball mill. *ACS Catal.* **2017**, *7*, 4592. (f) Liu, Y.; Xie, F.; Jia, A.-Q.; Li, X.-W.  $Cp^*Co(III)$ -catalyzed amidation of



olefinic and aryl C-H bonds: highly selective synthesis of enamides and pyrimidines. *Chem. Commun.* **2018**, *54*, 4345.

(10) Park, Y.; Chang, S. Asymmetric formation of  $\gamma$ -lactams via C-H amidation enabled by chiral hydrogen-bond-donor catalysts. *Nat. Catal.* **2019**, *2*, 219.

(11) Xing, Q.; Chan, C.-M.; Yeung, Y.-W.; Yu, W.-Y. Ruthenium(II)-catalyzed enantioselective  $\gamma$ -lactams formation by intramolecular C-H amidation of 1,4,2-dioxazol-5-ones. *J. Am. Chem. Soc.* **2019**, *141*, 3849.

(12) Wang, H.; Park, Y.; Bai, Z.; Chang, S.; He, G.; Chen, G. Iridium-catalyzed enantioselective C(sp<sup>3</sup>)-H amidation controlled by attractive noncovalent interactions. *J. Am. Chem. Soc.* **2019**, *141*, 7194.

(13) The rearrangement could alternatively be called a Lossen-type rearrangement. See: Aubé, J.; Fehl, C.; Liu, R.; McLeod, M. C.; Motiwala, H. F. 6.15 Hofmann, Curtius, Schmidt, Lossen, and Related Reactions. In *Comprehensive Organic Synthesis II* (Second ed.); Knochel, P., Ed.; Elsevier: Amsterdam, 2014; Vol. 6; pp 598–635.

(14) For a rare example of a coordination complex with a 7-alkyl-1,7-phenanthroline ligand, see: Song, G.; Zhang, Y.; Su, Y.; Deng, W.; Han, K.; Li, X. Pyridine-based N-heterocyclic carbene hydride complexes of iridium via C-H activation. *Organometallics* **2008**, *27*, 6193.

(15) Ligand **1** was synthesized following two different routes. See [Supporting Information](#) for more details.

(16) Lin, Z.; Celik, M. A.; Fu, C.; Harms, K.; Frenking, G.; Meggers, E. N-Sulfinylcarboximidates as a new class of chiral bidentate ligands: Application to asymmetric coordination chemistry. *Chem. - Eur. J.* **2011**, *17*, 12602.

(17) Gong, L.; Wenzel, M.; Meggers, E. Chiral-auxiliary-mediated asymmetric synthesis of ruthenium polypyridyl complexes. *Acc. Chem. Res.* **2013**, *46*, 2635.

(18) Coe, B. J.; Glenwright, S. J. Trans-effects in octahedral transition metal complexes. *Coord. Chem. Rev.* **2000**, *203*, 5.

(19) For a ruthenium complex with a protonated cyclometalated 1,7-phenanthroline, see: Fukushima, T.; Fukuda, R.; Kobayashi, K.; Caramori, G. F.; Frenking, G.; Ehara, M.; Tanaka, K. Proton-induced generation of remote N-heterocyclic carbene-Ru complexes. *Chem. - Eur. J.* **2015**, *21*, 106.

(20) Zhou, Z.; Chen, S.; Qin, J.; Nie, X.; Zheng, X.; Harms, K.; Riedel, R.; Houk, K. N.; Meggers, E. Catalytic Enantioselective intramolecular C(sp<sup>3</sup>)-H amination of 2-azidoacetamides. *Angew. Chem., Int. Ed.* **2019**, *58*, 1088.

(21) Qin, J.; Zhou, Z.; Cui, T.; Hemming, M.; Meggers, E. Enantioselective intramolecular C-H amination of aliphatic azides by dual ruthenium and phosphine catalysis. *Chem. Sci.* **2019**, *10*, 3202.

(22) Besides **6e** and **6f**, recrystallization was used to improve the er of the thiophene compound **6h**. See [Supporting Information](#) for more details.

(23) Substrates bearing nonbenzylic tertiary C-H bonds provided very low C-H amidation yields, and the corresponding Curtius rearrangement products were formed as the major products. See [Supporting Information](#) for more details.

(24) During the gram-scale transformation of substrate **5e** to lactam product **6e**, (S)-**6e** directly precipitates from the reaction solution, which can be easily separated from the reaction solution. The total yield can be further increased by cooling the solution to 0 °C. See [Supporting Information](#) for more details.

(25) Using the mirror-image catalyst  $\Delta$ -rNHCRu (0.005 mol%), (R)-**6e** was obtained under identical conditions with 54% yield and >99:1 er.

(26) Xue, Z.-Y.; Liu, L.-X.; Jiang, Y.; Yuan, W.-C.; Zhang, X.-M. Highly enantioselective Lewis base organocatalyzed hydrosilylation of  $\gamma$ -imino esters. *Eur. J. Org. Chem.* **2012**, *2012*, 251.

(27) Keusenkothen, P.-F.; Smith, M.-B. Asymmetric radical cyclization with pyroglutamate: synthesis of 7-substituted pyrrolizidines. *J. Chem. Soc., Perkin Trans. 1* **1994**, *17*, 2485.

(28) McAlonan, H.; Stevenson, P. Asymmetric synthesis of S-(+)-4-amino-5-hexynoic acid. *Tetrahedron: Asymmetry* **1995**, *6*, 239.

(29) For comparison, using alternatively a 1:1 mixture of nondeuterated and bis-deuterated substrates provided a competitive intermolecular KIE of 1.3. See [Supporting Information](#) for more details.

(30) (a) Milczek, E.; Boudét, N.; Blakey, S. Enantioselective C-H amination using cationic Ru(II)-pybox catalysts. *Angew. Chem., Int. Ed.* **2008**, *47*, 6825. (b) Fiori, K. W.; Espino, C. G.; Brodsky, B. H.; Du Bois, J. A mechanistic analysis of the Rh-catalyzed intramolecular C-H amination reaction. *Tetrahedron* **2009**, *65*, 3042. (c) Collet, F.; Lescot, C.; Liang, C.; Dauban, P. Studies in catalytic C-H amination involving nitrene C-H insertion. *Dalton Trans.* **2010**, *39*, 10401. (d) Harvey, M. E.; Musaev, D. G.; Du Bois, J. A diruthenium catalyst for selective, intramolecular allylic C-H amination: reaction development and mechanistic insight gained through experiment and theory. *J. Am. Chem. Soc.* **2011**, *133*, 17207. (e) Nguyen, Q.; Sun, K.; Driver, T. G. Rh<sub>2</sub>(II)-catalyzed intramolecular aliphatic C-H bond amination reactions using aryl azides as the N-atom source. *J. Am. Chem. Soc.* **2012**, *134*, 7262. (f) Bon, J. L.; Blakey, S. B. Synthesis of Ruthenium(II) 2,6-bis(imino)pyridyl complexes for C-H amination of sulfamate esters. *Heterocycles* **2012**, *84*, 1313. (g) Alderson, J. M.; Phelps, A. M.; Scamp, R. J.; Dolan, N. S.; Schomaker, J. M. Ligand-controlled, tunable silver-catalyzed C-H amination. *J. Am. Chem. Soc.* **2014**, *136*, 16720. (h) Alt, I. T.; Guttroff, C.; Plietker, B. Iron-catalyzed intramolecular C(sp<sup>3</sup>)-H amination. *Angew. Chem., Int. Ed.* **2016**, *55*, 1519. (i) Li, C.; Lang, K.; Lu, H.; Hu, Y.; Cui, X.; Wojtas, L.; Zhang, X. P. Catalytic radical process for enantioselective amination of C(sp<sup>3</sup>)-H bonds. *Angew. Chem., Int. Ed.* **2018**, *57*, 16837. (j) Clark, J. R.; Feng, K.; Sookezian, A.; White, M. C. Manganese-catalyzed benzylic C(sp<sup>3</sup>)-H amination for late-stage functionalization. *Nat. Chem.* **2018**, *10*, 583. (k) Shing, K.-P.; Liu, Y.; Cao, B.; Chang, X.-Y.; You, T.; Che, C.-M. *Angew. Chem., Int. Ed.* **2018**, *57*, 11947.

(31) For selected examples on nitrene transfer to phosphines, see: (a) Sleiman, H. F.; Mercer, S.; McElwee-White, L. Tapping of the low-valent nitrene complex (CO)<sub>5</sub>W = NPh with PPh<sub>3</sub>. Formation of the phenylnitrene transfer product PhN = PPh<sub>3</sub>. *J. Am. Chem. Soc.* **1989**, *111*, 8007. (b) Harlan, E. W.; Holm, R. H. Molybdenum-mediated imido group transfer: stoichiometric and catalytic reactions and structures. *J. Am. Chem. Soc.* **1990**, *112*, 186. (c) Dobbs, D. A.; Bergman, R. H. Synthesis of bridging iridium bis(imido) and imido-oxo complexes. Imide and oxygen transfer reactions and hydrogenation of an imido ligand. *J. Am. Chem. Soc.* **1993**, *115*, 3836. (d) Perez, P. J.; White, P. S.; Brookhart, M.; Templeton, J. L. Nitrene transfer to trimethylphosphine from cationic tungsten tosyl nitrene complexes [Tp'(CO)2W(NTs)]<sup>+</sup>[X]<sup>-</sup>. *Inorg. Chem.* **1994**, *33*, 6050.

(32) (a) Zabalov, M. V.; Tiger, R. P. Why Lewis acids accelerate the thermal Curtius rearrangement of benzoyl azide into phenyl isocyanate. *J. Mol. Struct.: THEOCHEM* **2010**, *962*, 15. (b) Kakkar, R.; Arora, R.; Zaidi, S. DFT studies on the acid-catalyzed Curtius reaction: the Schmidt reaction. *Struct. Chem.* **2017**, *28*, 1743.

(33) On the other hand, a recent study by Chang and co-workers revealed that a concerted and asynchronous decarboxylation of the dioxazolone is taking place when the filled d<sub>yz</sub> orbital of the transition metal catalyst overlaps with the nitrogen p<sub>z</sub> orbital in the course of the transition metal imido intermediate formation. See: Park, Y.; Heo, J.; Baik, M.-H.; Chang, S. Why is the Ir(III)-mediated amido transfer much faster than the Rh(III)-mediated reaction? A combined experimental and computational study. *J. Am. Chem. Soc.* **2016**, *138*, 14020.

(34) Determined Ru(II/III) redox potentials for the investigated ruthenium catalysts (rNHCRu, Ru2, Ru3: 0.90 V; Ru4, Ru5, Ru6: 1.33 V vs Ag/AgCl in MeCN) are consistent with a more electron-rich ruthenium center for the complexes bearing rNHC ligands.

(35) Anderson, K. M.; Orpen, A. G. On the relative magnitudes of cis and trans influences in metal complexes. *Chem. Commun.* **2001**, *203*, 2682.

(36) We were able to experimentally verify that the *trans* effect results in differential lability of the nitrile ligands in C<sub>2</sub>-symmetric and non-C<sub>2</sub>-symmetric catalysts. For C<sub>2</sub>-rNHCRu, both nitriles are labile

due to being positioned *trans* to rNHC carbene carbons. In rNHCRu, only one nitrile is labilized. See [Supporting Information](#) for more details.

(37) The computed triplet pathway for hydrogen atom abstraction is consistently 4–5 kcal/mol higher in energy than the singlet pathway. The closed-shell singlet structures of the Ru nitrenes are the lowest-energy state for **8a**, **8b**, and **8c**. As such, our calculations do not lend support to the idea that a crossover from a singlet to a triplet mechanism is responsible for the C–H amidation versus Curtius rearrangement selectivity.

(38) For a recent report on an enzymatic enantioselective intramolecular C–H amidation with acyl-protected hydroxamate precursors at very low catalyst loadings, see: Inha, C.; Jia, Z.-J.; Arnold, F. H. Site-selective enzymatic C-H amidation for synthesis of diverse lactams. *Science* **2019**, 364, 575.